

# In-Chain Tunneling Through Charge-Density Wave Nanoconstrictions

K. O'Neill, E. Slot, and H. S. J. van der Zant

*Kavli Institute of Nanoscience Delft, Delft University of Technology, Lorentzweg 1, 2628 CJ Delft, The Netherlands*

R. E. Thorne

*Laboratory of Atomic and Solid State Physics, Cornell University, Ithaca, New York 14853*

(Dated: 5<sup>th</sup> September 2005)

We have fabricated longitudinal nanoconstrictions in the charge-density wave conductor (CDW)  $\text{NbSe}_3$  using a mechanically controlled break-junction technique and by employing a focused ion beam. Conductance peaks are observed at  $190 \pm 6$  meV and  $106 \pm 6$  meV below the  $T_{P1} = 145$  K and  $T_{P2} = 59$  K CDW transitions, respectively. These values correspond closely with previous values of the full CDW gaps  $2\Delta_1$  and  $2\Delta_2$  obtained from different experimental techniques. No conductance peaks are observed below  $T_{P2}$  at  $\Delta_1 + \Delta_2$ , which would be expected in CDW-CDW tunneling between two peaks in the density of states. These results can be explained by assuming CDW-CDW tunneling in the presence of an energy gap corrugation  $\epsilon_2$  comparable to  $\Delta_2$ , or by assuming tunneling through back-to-back CDW-normal junctions.

Charge-density wave (CDW) conduction remains of major interest despite its experimental discovery nearly 30 years ago. Much of the existing work has focused on transport properties of as-grown single crystals [1]. More recently, the development micro/nanofabrication methods for CDW materials has allowed the study of mesoscopic CDW physics. [2, 3]. Structures for tunneling spectroscopy are of particular interest because of the unusual gap structure with large one-dimensional fluctuation effects expected in these highly anisotropic materials, and because of predictions of unusual mid-gap excitations of the collective mode [4]. Tunneling studies in fully gapped CDW conductors like the "blue bronze"  $\text{K}_{0.3}\text{MoO}_3$  suffer from band-bending effects at the interface akin to semiconductor-insulator-metal junctions. These effects are absent in the partially gapped CDW conductor  $\text{NbSe}_3$ , which remains metallic down to 4.2 K.

Scanning tunneling microscopes have been used to study tunneling perpendicular to the quasi-one-dimensional chains, along which the CDW wavevector lies, in ribbon-like whiskers of  $\text{NbSe}_3$ . [5]. In-chain tunneling studies have used metal [6] or  $\text{NbSe}_3$  [7] "tips" mechanically positioned near the end of a crystal, and only the latter have simultaneously shown tunneling peaks at  $\Delta_1$  and  $\Delta_2$ . Because they involve native crystal surfaces, such mechanical point contacts have poor stability [2].

Here we demonstrate that a small constriction in a  $\text{NbSe}_3$  single crystal, produced by dry etching with a Ga Focused Ion Beam (FIB), shows tunneling peaks at  $2\Delta_1$  and  $2\Delta_2$ , as illustrated in Figure 1. We reproduce the data at 4.2 K using a Mechanically Controlled Break-Junction (MCBJ) technique, demonstrating that the FIB results are not dominated by Ga ion damage or implantation. Our results can be explained either by CDW-CDW tunneling in the presence of a large transverse gap corrugation, or by back-to-back CDW-normal tunneling.

CDWs form in metals with quasi-one-dimensional Fermi surfaces. Electron-hole pairs near the Fermi level  $k_F$  form a macroscopic condensate and associated periodic modulations of the electron density and atomic po-

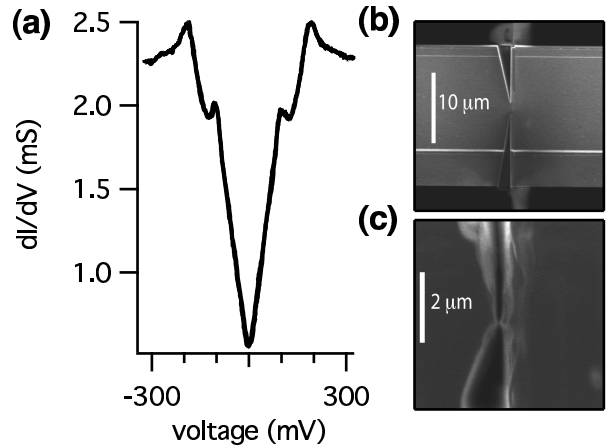


FIG. 1: (a) Differential conductance  $\frac{dI}{dV}$  vs applied voltage at  $T = 4.2$  K of a FIB-fabricated  $\text{NbSe}_3$  nanoconstriction. (b) and (c) show images taken in the FIB during fabrication.

sitions. The condensate arises from the electron-phonon interaction, as described by the mean-field Hamiltonian  $H_P = \sum_{k\sigma} \epsilon_k a_{k\sigma}^\dagger a_{k\sigma} - \sum_{k\sigma} (a_{k\sigma}^\dagger a_{k+k_F\sigma} \Delta e^{i\phi} + h.c.)$  [9], where  $a_{k\sigma}$  ( $a_{k\sigma}^\dagger$ ) is the electron creation (annihilation) operator for the states with wavevector  $k$  and spin  $\sigma$ . Like conventional superconductors, the CDW condensate produces peaks in the density-of-states (DOS) at  $\pm\Delta$  relative to the Fermi energy. Applying the semiconductor model for electron tunneling in superconductor junctions [10] to CDW systems, tunneling between occupied and unoccupied states in a CDW-insulating-CDW junction should produce peaks in the conductance at voltages equal to  $\pm\frac{2\Delta}{e}$ . In a CDW-normal junction, peaks should be observed at voltages equal to  $\pm\frac{\Delta}{e}$ .

To fabricate nanoconstrictions using the FIB, a single-crystal whisker of  $\text{NbSe}_3$  with a typical width of 20  $\mu\text{m}$  was placed on a silicon dioxide/silicon substrate having

2  $\mu\text{m}$  wide electrical Au contacts that were pre-patterned by photolithographic techniques. The  $\text{NbSe}_3$  crystal was then carved using an FEI/Philips FIB-200 focused ion beam. At low magnification ( $10,000\times$ ), two large transverse cuts were made from either side to create a constriction in the  $\mathbf{b}/\mathbf{b}^*$  direction. At high magnification ( $50,000\times$ ), further line cuts were made at low currents of 350 pA until the constriction had a width of around 100 nm and its resistance (which dominated the overall sample resistance) exceeded  $150\Omega$  at room temperature. Images of both cuts, taken in the FIB, are shown in Figure 1(b). Differential conductance versus voltage data was measured between  $T_P = 145\text{ K}$  and 4.2 K using a conventional four-probe technique.

To fabricate constrictions by the mechanically-controlled break-junction technique, a single crystal whisker of  $\text{NbSe}_3$  was placed on a Kapton-tape capped piece of flexible phosphor-bronze. The crystal was controllably broken at 4.2 K in a custom-built cryostat [12], which allowed the sample to be broken and re-contacted several times in the course of an experiment. Cellulose held the crystal in electrical contact with gold pads pre-patterned onto the Kapton. Transport measurements at  $T=4.2\text{ K}$  were performed in two-probe configuration, with a contact resistance of  $\sim 10\Omega$  estimated from the total resistance total sample plus contact resistance before breaking. Because of the quasi-one-dimensional bonding and very strong bonds along the chains, the response of  $\text{NbSe}_3$  crystal to stress likely involved successive breaking of fibers within its cross-section, as in the breaking of a rope.

Figure 2(a) shows that the zero-bias resistance of the constriction increases monotonically with decreasing temperature, and at 4.2 K has a value close to  $2\text{k}\Omega$ . This contrasts with the bulk behavior of  $\text{NbSe}_3$ , which shows large resistance increases just below the two Peierls transitions and then a strong metallic (roughly linear) decrease down to 4.2 K, suggesting a fundamental change in the character of transport through the constriction. Using the Sharvin resistance formula for point contacts [13] and the value for the electron density in  $\text{NbSe}_3$  at temperatures below 40 K [15], the measured low-temperature resistance implies a contact area of roughly 60 nm. Alternatively, using the room temperature resistance of the contact ( $165\Omega$ ), the bulk resistivity of  $\text{NbSe}_3$  ( $1.86\Omega\mu\text{m}$ ), a contact length of around 100 nm (estimated from the device image in Figure 1(b)), and the bulk resistance formula gives a conducting area of roughly 20 nm, in order-of-magnitude agreement with the Sharvin estimate. Part of the difference may be due to additional resistance caused by charge flow through the much larger transverse resistivity as it approaches the constriction.

Figure 2(b) shows the differential conductance of the FIB sample as a function of voltage for several temperatures, with the lowest temperature differential conductance offset downwards for clarity. At  $T=4.2\text{ K}$ , peaks occur at  $\pm 105\text{ mV}$  and  $\pm 190\text{ mV}$ , symmetric around zero bias, with an estimated error  $\sim 6\text{ mV}$  and width

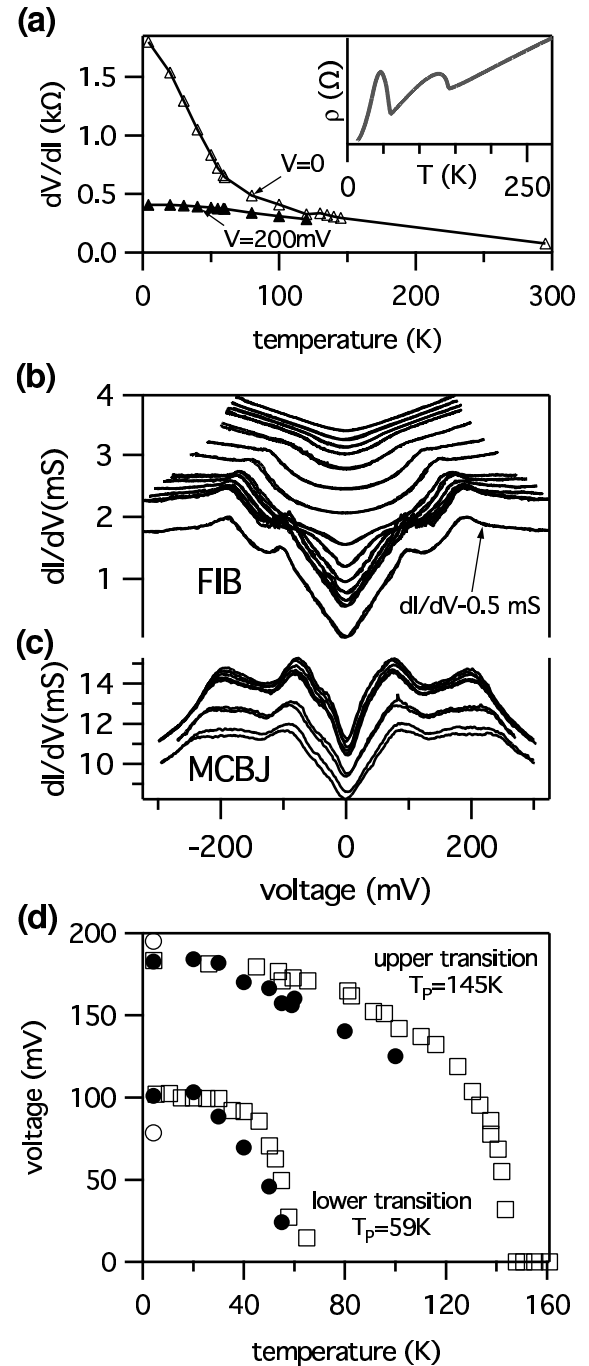


FIG. 2: (a)  $\frac{dI}{dV}$  of the FIB nanoconstriction at  $V = 0\text{ mV}$  and  $V = 200\text{ mV}$  as a function of temperature. Anomalies due to the two Peierls transitions at  $145\text{ K}$  and  $59\text{ K}$  seen in the bulk resistivity (inset) are absent. (b)  $\frac{dI}{dV}$  vs voltage of the FIB constriction at temperatures (top to bottom) of 4.2 K, 20 K, 30 K, 40 K, 50 K, 80 K, 100 K, 120 K, 130 K, 135 K, 140 K and 145 K. The 4.2 K data is repeated, offset downward by  $-0.5\text{ mS}$ , for clarity. (c)  $\frac{dI}{dV}$  vs voltage of the break-junction sample taken at different stresses/separations. (d) Peak positions obtained from the FIB constriction data of (b) (filled circles) and from the MCBJ data of (c) (open circles), compared with temperature dependence of the CDW gap determined from X-ray data [14] (open squares).

$\sim 30$  meV. The peak positions move to smaller voltage with increasing temperature. Above its corresponding  $\sim 2T_P/3$ , each peak becomes an inflection, and above  $T_P$  each inflection disappears, indicating a strict association of each peak with each Peierls instability. Figure 2(c) shows the corresponding data at  $T = 4.2$  K from the MCBJ sample. Peaks are clearly visible at  $\pm 81$  mV and  $\pm 196$  mV.

The agreement between the MCBJ and FIB samples indicate that the transport properties of the FIB samples are not qualitatively changed by any damage or disorder caused by Gallium atoms. The measured  $T = 4.2$  K peak positions correspond well to recent angle-resolved photo-emission spectroscopy measurements of the CDW gaps of 90 and 220 meV, respectively [16]. Figure 2(d) shows the position of the conduction peaks (or inflections) with temperature. The data closely match X-ray data Fleming *et al.* [14] for the temperature dependence of the CDW gap, when scaled to the values at 4.2 K. The qualitative and quantitative features of our data indicate that the observed peaks are due to tunneling involving CDW states near NbSe<sub>3</sub>'s two gaps. In both the FIB and MCBJ samples small features at  $\sim 60$  mV are observed, possibly due to soliton effects [4]. No samples show any feature at  $\frac{\Delta_1 + \Delta_2}{e} = 148$  meV, expected for tunneling between the two different CDWs.

Our measurements show that the conductance peak widths do not significantly vary below  $\frac{T_P}{2}$  for either transition, implying a temperature-independent intrinsic broadening of the CDW DOS. The conductance also shows a substantial tail as the voltage decreases below the gap, indicating that the DOS does not cut off sharply below the gap down to the lowest temperatures. This is consistent with optical absorption measurements [17], and calculations of the zero-temperature CDW DOS with one-dimensional fluctuations [19]. The suppression of conductance peaks at  $> 2T_P/3$  for each transition is likely due to the strong effect of thermal fluctuations in a quasi-one-dimensional system, in agreement with calculations of the DOS near the Peierls transition [20]. Both the low and high temperature behaviors underline the strong role that fluctuation effects play in CDW systems.

Our results may be explained in terms of CDW-CDW tunneling in the presence of a transverse corrugation of the  $T_{P2}$  CDW's energy gap, as shown in Figure 3. A transverse corrugation of the  $T_{P2}$  gap larger than the gap itself has been suggested based on the low-bias behavior of metal-NbSe<sub>3</sub> tunnel junctions and on comparison of thermal and electric conduction at low temperatures [6, 8]. We consider a semiconductor tunneling model [10] that incorporates dispersion of the quasiparticle states in momenta perpendicular to the chains, arising from the finite transverse interchain coupling that results in imperfect Fermi surface nesting [11]. This dispersion is characterized by a single parameter  $\epsilon_0 = \frac{t_{\perp}^2 \cos(bk_F)}{2t_b \sin(bk_F)}$ ,  $t_{\perp}$  and  $t_b$  being the bandwidths of the dispersion perpendicular and parallel to the chains, and  $b$  the inter-chain separation. Figure 3(a) illustrates this dispersion, showing by bright-

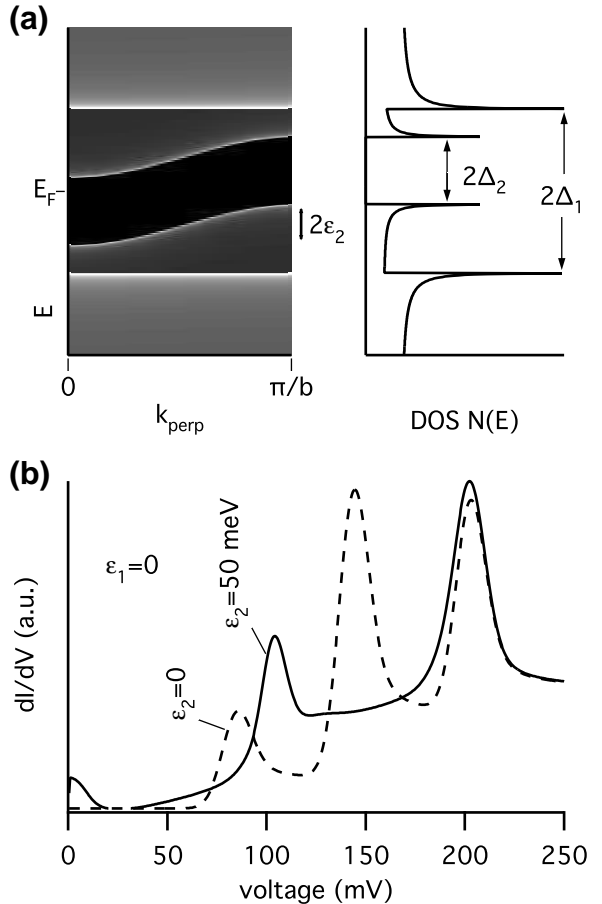


FIG. 3: Semiconductor model for transitions between quasi-particle excited states of the CDW, with corrugation  $\epsilon_2$  present in the transverse momentum direction of the  $T_{P2} = 59$  K but not the  $T_P = 145$  K CDW states: (a) left: Density of states  $N(E, k_{\perp})$  as a function of perpendicular wavevector and energy, showing how corrugation of the  $T_{P2}$  CDW changes the relative positions of the DOS maxima. Brighter regions denote higher DOS; right: Projection of  $N(E, k_{\perp})$  at a fixed wavevector  $k_{\perp} = \frac{\pi}{b}$ ; (b) Simulated  $\frac{dI}{dV}$  vs.  $V$  using BCS density of states broadened by 24 meV, and a corrugation  $\epsilon_2 = 0$  and 50 meV. All calculations assume  $\Delta_1 = 100$  meV and  $\Delta_2 = 41$  meV.

ness the density of states  $N(E, k_{\perp})$  as a function of energy and perpendicular wave vector within one half Brillouin zone (left), and the density of states at a  $N(E)$  at a fixed wavevector (right). The conductance is then calculated by integrating the product  $N(E, k_{\perp})N(E - eV, k_{\perp})$  over all energies  $E$  and wavevectors  $k_{\perp}$ , assuming a BCS  $T = 0$  DOS broadened by a Gaussian distribution with the experimentally measured width  $\sigma = 24$  meV. The computed  $\frac{dI}{dV}(V)$  curves for  $\epsilon_2 = 0$  (no corrugation) and  $\epsilon_2 = 50$  meV are shown in Figure 3(b). As expected, with no corrugation  $\frac{dI}{dV}(V)$  exhibits a strong peak at precisely  $(\Delta_1 + \Delta_2)/e$ . As  $\epsilon_2$  is increased, this peak splits in energy and shrinks in height. While all conductance peaks remain visible with a divergent DOS, with a broad-

ened DOS the peaks at  $\Delta_1 + \Delta_2 - \epsilon_2$  and  $2\Delta_2$  merge at around 100 meV, resulting in a conductance curve that closely resembles the present data. The predicted shift of the lower conductance peak associated with the  $T_{P2}$  gap also explains why our measured value of  $\frac{\Delta_2}{\Delta_1} = 0.55$  is higher than its expected value of  $\frac{T_2}{T_1} = 0.41$ , confirmed by ARPES measurements [16].

Estimates of  $\epsilon_2$  for the  $T_{P2}$  CDW based on electron tunneling in the crystallographic  $a^*$  direction and electronic band structure calculations [6] yield a value of around 10 meV. With the measured electrical anisotropy of NbSe<sub>3</sub> [21] this implies a value of roughly 50 meV for the other transverse ( $c$ ) direction. However, these calculations use the mean-field value for the gap of 8.5 meV, obtained from an incorrect interpretation of early optical measurements [22, 23]; more recent optical measurements [17] and ARPES measurements yield a gap 5× larger [16]. The corrugation we assume is in agreement with the conclusion of Sorbier *et al.* [6] that the corrugation for the  $T_{P2}$  CDW  $\epsilon_2$  is slightly larger than the energy gap  $\Delta_2$ .

An alternative explanation for the peak structure observed here is that CDW order is suppressed in the constriction (as has been suggested in measurements on CDW nanowires [24]). The resulting normal (N) region produces back-to-back N-CDW junctions. Provided that the relaxation length of the non-equilibrium distributions is long compared with the characteristic length of the transition from CDW to normal states, one would expect  $\frac{dI}{dV}$  peaks corresponding to just  $2\Delta_1$  and  $2\Delta_2$ , and no intermediate peak, consistent with our data. However, in NbSe<sub>3</sub> nanowires with cross-sectional areas as small as 500 nm<sup>2</sup>, the zero-bias temperature dependence

still exhibits hints of anomalies at the two Peierls transitions, whereas the FIB structure shows no evidence of such anomalies. Moreover, the relevance of this explanation to the MCBJ sample, where the sample has simply been broken and brought back close together, is unclear. For both the FIB and MCBJ structures, the microscopic structure that gives rise to the observed peaks is unknown.

In conclusion, we report that an in-chain CDW-CDW nanoconstriction has been fabricated that behaves like a tunnel junction and demonstrates peaks in the low temperature conductance in agreement with values for the energy gaps  $2\Delta_1$  and  $2\Delta_2$  previously reported in the literature. This device is reproducible and does not suffer from the mechanical instabilities reported with other types of point contacts [2]. The peaks disappear at around two-thirds the transition temperature, in agreement with calculations of fluctuation effect in the DOS for one-dimensional compounds.

We thank S. Zaitsev-Zotov and S. Artemenko for fruitful discussions. This work was supported by the International Association for the Promotion of Co-operation with Scientists from the New Independent States of the Former Soviet Union (INTAS-NIS), the Foundation for Fundamental Research on Matter (FOM), and the National Science Foundation (NSF) (Grants No. DMR 0101574 and No. INT 9812326). K.O'N. was supported by the Marie Curie Fellowship organization. We thank J. van Ruitenbeek for the use of equipment in the MCBJ work, and S. Otte and R. Thijssen for technical assistance.

---

[1] G. Grüner, Rev. Mod. Phys. **60**, 1129 (1988).  
 [2] A. A. Sinchenko, Y. I. Latyshev, S. G. Zybttsev, I. G. Gorlova and P. Monceau, Phys. Rev. B **60**, 4624 (1999); Y. I. Latyshev *et al.*, J. Phys. A: Math. Gen. **36**, 9323 (2003).  
 [3] S. V. Zaitsev-Zotov, Physics-Uspekhi **6**, 533 (2004); S. V. Zaitsev-Zotov, V. Y. Pokrovski, and P. Monceau, JETP letters **73**, 25, (2001).  
 [4] S. Brazovskii, I. E. Dzyaloshinskii and I. M. Krichever, Physics Letters A **91**, 40 (1982).  
 [5] Z. Dai, C. G. Slough, and R. V. Coleman, Phys. Rev. B **45**, R9469 (1992).  
 [6] J. P. Sorbier, H. Tortel, P. Monceau and F. Levy, Phys. Rev. Lett. **76**, 676 (1996).  
 [7] T. Ekino and J. Akimitsu, Japanese Journal of Applied Physics **26**, 625 (1987).  
 [8] G. Mihály, A. Virosztek, and G. Grüner, Phys. Rev. B **55**, R13456 (1997).  
 [9] H. Fröhlich, Proc. R. Soc. London Ser. A **223** (1954); R. E. Peierls, *Quantum Theory of Solids* (Oxford University Press, 1955).  
 [10] G. E. Blonder, M. Tinkham, and T. M. Klapwijk, Phys. Rev. B **25**, 4515 (1982).  
 [11] X. Huang and K. Maki, Phys. Rev. B **42**, 6498 (1990);  
 X. Z. Huang and K. Maki, Phys. Rev. B **40**, 2575 (1989).  
 [12] J. M. van Ruitenbeek *et al.*, Rev. Sci. Instrum. **67**, 108 (1996).  
 [13] Y. Sharvin, JETP **21**, 665 (1965).  
 [14] R. M. Fleming, D. E. Moncton, and D. B. McWhan, Phys. Rev. B **18**, 5560 (1978).  
 [15] N. P. Ong, Phys. Rev. B **18**, 5272 (1978).  
 [16] J. Schäfer *et al.*, Phys. Rev. Lett. **91**, 066401 (2003).  
 [17] A. Perucchi, L. Degiorgi, and R. E. Thorne, Phys. Rev. B **69**, 195114 (2004).  
 [18] L. Degiorgi *et al.*, Phys. Rev. B **52**, 5603 (1995).  
 [19] K. Kim, R. H. McKenzie, and J. W. Wilkins, Phys. Rev. Lett. **71**, 4015 (1993); R. H. McKenzie and J. W. Wilkins, Phys. Rev. Lett. **69**, 1085 (1992).  
 [20] P. A. Lee, T. M. Rice, and P. W. Anderson, Phys. Rev. Lett. **31**, 462 (1973).  
 [21] N. P. Ong and J. W. Brill, Phys. Rev. B **18**, 5265 (1978); E. Slot, H. S. J. van der Zant, and R. E. Thorne, Phys. Rev. B **65**, 033403 (2001).  
 [22] W. A. Challener and P.L. Richards, Solid State Communications **52**, 117 (1984).  
 [23] The optical measurements by Challener and Richards [22] do not extend to energies large enough to measure absorption at 43 meV or greater, less than half  $2\Delta_2$ .

[24] E. Slot *et al.*, Phys. Rev. Lett. **93**, 176602 (2004).